Solar Energy Materials & Solar Cells 94 (2010) 22–28

Contents lists available at ScienceDirect

Solar Energy Materials & Solar Cells

journal homepage: www.elsevier.com/locate/solmat

Enhanced spectral response in polymer bulk heterojunction solar cells by using active materials with complementary spectra ☆

Jen-Hsien Huang [a], Chuan-Pei Lee [a], Zhong-Yo Ho [b], Dhananjay Kekuda [c], Chih-Wei Chu [c,d,*], Kuo-Chuan Ho [a,b,1]

[a] Department of Chemical Engineering, National Taiwan University, Taipei 10617, Taiwan
[b] Institute of Polymer Science and Engineering, National Taiwan University, Taipei 10617, Taiwan
[c] Research Center for Applied Sciences, Academia Sinica, 128, Section 2, Academia Road, Nankang, Taipei 11529, Taiwan
[d] Department of Photonics, National Chiao Tung University, Hsinchu 300, Taiwan

ARTICLE INFO

Article history:
Received 31 August 2008
Received in revised form
4 February 2009
Accepted 15 February 2009
Available online 13 March 2009

Keywords:
Polymer solar cell
Polyfluorene
PCBM
Spectra coverage
Bulk heterojunction

ABSTRACT

We have fabricated organic photovoltaic devices with blends of poly[9,9′-dioctyl-fluorene-*co*-bithiophene] (F8T2) and fullerene as an electron donor and electron acceptor, respectively. A significant improvement of the photovoltaic efficiency was found in device by using active materials with complementary spectra. The different weight ratios of composite film were also performed to correlate between morphology and the device performance. A power conversion efficiency (PCE) up to 2.0% with an open-circuit voltage of 0.85 V and a short-circuit current (J_{SC}) of 5.3 mA/cm^2, was achieved by blending the F8T2 with [6,6]-phenyl-C71-butyric acid methyl ester (PC[70]BM).

1. Introduction

In recent years, solar cells as a promising source of renewable and truly clean energy have become more and more attractive. Driven by the demand for inexpensive, clean, and renewable energy sources, the field of organic solar cells has grown as a result of their potential low cost, ease of processing, and the feasibility of fabricating on various substrates [1]. Until now, power conversion efficiency (PCE) up to 5% has been achieved from the bulk heterojunction (BHJ) of poly(3-hexylthiophene) (P3HT) blended with [6,6]-phenyl-C61-butyric acid methyl ester (PC[60]BM) [2]. Although the transport properties have been dramatically improved by vertical phase separation of both donor and acceptor, they still lack the absorption in the red and infrared regions [3]. Therefore, great deal of efforts have been undertaken to enhance the J_{SC} of solar cells by utilizing low bandgap-conjugated polymers [4,5]. Indeed, the absorption spectra have been shifted by employing such low bandgap polymers. However, the low mobility limited the thickness of photoactive layer, resulting in weak absorption. Moreover, the power conversion efficiency was also limited by the fixed V_{OC} determined by the difference between the highest occupied molecular orbital (HOMO) of donor and lowest unoccupied molecular orbital (LUMO) of acceptor [6].

Polyfluorene (PF) copolymers are well known for their high charge carrier mobility [7–10], and the versatility of chemical structure. Recently, the BHJ polymer solar cells with larger V_{OC} (0.9–0.95 V) using PF-based alternating copolymers as donor have been reported [11–16]. For example, F8T2 has well been explored in the area of organic field-effect transistors, with good hole transporting properties. They exhibit excellent thermo tropic liquid crystallinity, which allows better chain packing via self-assembly [8,16]. On the basis of the result, it is expected that the charge transport in F8T2:PC[60]BM can be strongly balanced. Although, the polymer only absorbs light at wavelengths less than 500 nm which reduces the photocurrent dramatically [17], the absorption in the blue region of F8T2 make it an excellent donor polymer to blend with an acceptor having complementary spectrum or assemble a tandem cell with other low bandgap-conjugated polymers with absorption extended in the red region.

☆ This paper (S4-P45) was presented at the International Materials Research Congress (IMRC), Symposium 4-Photovoltaics, Solar Energy Materials and Thin Films, August 17–21, 2008, Cancun, Mexico, and submitted for consideration of publication in *Solar Energy Materials and Solar Cells*.

* Corresponding author at: Research Center for Applied Sciences, Academia Sinica, 128, Section 2, Academia Road, Nankang, Taipei 11529, Taiwan.
Tel.: +886 2789 8000x70; fax: +886 2 2782 6680.
E-mail addresses: gchu@gate.sinica.edu.tw (C.-W. Chu), kcho@ntu.edu.tw (K.-C. Ho).
[1] Also for correspondence. Tel.: +886 2 2366 0739; fax: +886 2 2362 3040.

0927-0248/$ - see front matter © 2009 Elsevier B.V. All rights reserved.
doi:10.1016/j.solmat.2009.02.019

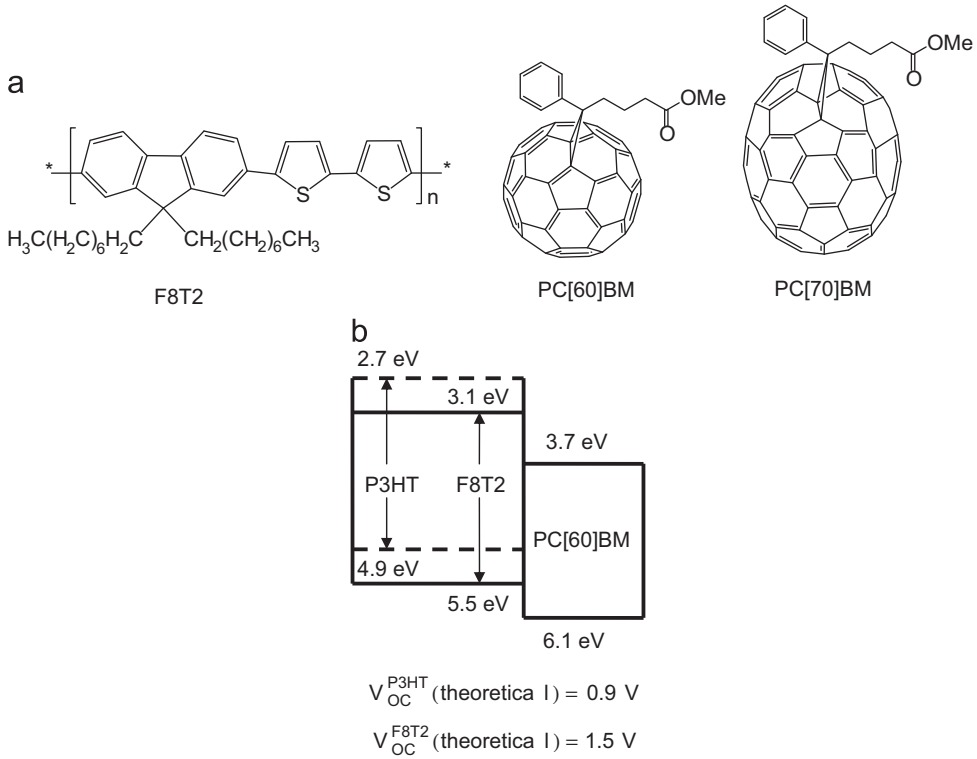

Fig. 1. (a) Chemical structures of F8T2, PC[60]BM, and PC[70]BM. (b) Energy-level diagrams of F8T2:PC[60]BM and P3HT:PC[60]BM mixed films.

Therefore, it appears to be one of the most promising candidates among the conjugated polymers for high-efficiency polymer solar cells.

Recently, an approach to extend the photocurrent spectrum has been proposed by changing the acceptor in the BHJ solar cell, except utilizing a low bandgap polymer. The cell efficiency of the poly[2-methoxy-5-(3′,7′-dimethyloctyloxy)-*p*-phenylenevinylene](MDMO-PPV):PCBM photovoltaic (PV) device could be improved to 3% by replacing the PC[60]BM with PC[70]BM [18]. Other blending systems were also reported [19,20]. This enhancement can be contributed to the broader and higher absorption of PC[70]BM compared with that of PC[60]BM. The low absorption coefficient of PC[60]BM can be attributed to a high degree of symmetry which forbids the lowest energy transition. Therefore, when the PC[60]BM is replaced by a less symmetrical fullerene, namely PC[70]BM, the transition will become apparent and a significant increase in light absorption can be expected [21]. In this letter, we report an increase of efficiency from 1.4% to 2.0% in BHJ solar cell of F8T2 blended with complementary acceptor, PC[70]BM, to replace the analogous PC[60]BM which possesses a very low absorption coefficient in the visible range of the spectrum.

2. Experimental

The polymer PV cells in this study consists of a layer of F8T2:PCBM blend thin film sandwiched between transparent anode indium tin oxide (ITO) and metal cathode. The F8T2 was purchased from American Dye Source. The average molecular weight of F8T2 is 1×10^4. The PCBM was purchased from Nano-C (99%). Before device fabrication, the ITO glasses ($1.5\times1.5\,cm^2$) were ultrasonically cleaned in detergent, de-ionized water, acetone, and isopropyl alcohol before the deposition. After routine solvent cleaning, the substrates were treated with UVO (ultraviolet ozone cleaner, Jelight Company, USA) for 15 min. Then a modified ITO surface was obtained by spin-coating a layer of poly(ethylene dioxythiophene): polystyrenesulfonate (PEDOT:PSS) (~30 nm). After baking at 130 °C for 1 h, the substrates were then transferred into a nitrogen-filled glove box. The polymer PV devices were fabricated by spin-coating blend of F8T2:PCBM on the PEDOT:PSS modified ITO surface. Prior to the deposition, the blend of F8T2:PCBM was prepared by dissolving it in 1,2-dichlorobenzene with various weight ratios, followed by stirring the solution for 12 h at 50 °C. The active layer was obtained by spin-coating the blend at 600 rpm for 60 s. The active layer was then dried in covered glass Petri dishes to control the film growth rate. Subsequently, the films were annealed on the top of hotplate at various temperatures for 20 min. A 30 and 100 nm thick of calcium and aluminum was thermally evaporated under vacuum at a pressure below 6×10^{-6} Torr thorough a shadow mask. The active area of the device was 0.12 cm^2.

Current–voltage (*J*–*V*) characteristics were measured in the glove box under nitrogen atmosphere with simulated AM 1.5 G irradiation at 100 mW/cm^2 using a xenon lamp-based solar simulator (Thermal Oriel 1000 W). The light intensity was calibrated by a crystalline-silicon photodiode with KG-5 color filter (Hamamatsu, Inc.). For measuring absorption properties of polymer films, samples were fabricated on a glass substrate. The UV–visible absorption spectra were measured using a Jasco-V-670 UV–visible spectrophotometer. Surface morphologies were observed by an atomic force microscopy (AFM, Digital instrument NS 3a controller with D3100 stage). The thickness of all polymer films was measured using a surface profiler. The external quantum efficiency (EQE) spectrum was obtained at the short-circuit condition. The light source employed for the EQE measurements was a 450 W Xe lamp (Oriel Instrument, model 6266) equipped with a water-based IR filter (Oriel Instrument, model 6123 NS). The light output from the monochromator (Oriel Instrument, model 74,100) was focused onto the photovoltaic cell under test. The effective range of the monochromator was 190–900 nm. The EQE(λ) is defined as $EQE(\lambda)=1240(J_{SC}/\lambda\Phi)$, where λ is the wavelength, J_{SC} the short-circuit photocurrent (mA/cm^2) recorded

with a potentiostat/galvanostat (PGSTAT 30, Autolab, Eco-Chemie), and Φ the incident radiative flux (W/m^2) measured with an optical detector (Oriel Instrument, model 71580) and power meter (Oriel Instrument, model 70310). The factor 1240 is derived from hc/q, where h is the Plank's constant, c the speed of light, and q the electron charge. This curve can be derived from the measured absorption spectrum of the photosensitizer for comparison.

3. Results and discussions

Fig. 1 (a) presents the structures of F8T2, PC[60]BM, and PC[70]BM. The energy-level diagram of the HOMO and LUMO of F8T2 compared with that of PC[60]BM is shown in Fig. 1(b). The bandgap offset between the LUMOs of donor and acceptor is enough for electrons to be driven forward. Furthermore, the V_{OC} of devices based on a blend of a donor and PCBM can be predicted by $V_{oc} = \frac{1}{e}([E^{Donor}_{HOMO}] - [E^{PCBM}_{LUMO}]) - 0.3$, as suggested by Scharber et al. [6]. Apparently, larger V_{OC} can be achieved in the case of F8T2:PCBM compared with that of the P3HT:PCBM solar cells due to the lower HOMO level of F8T2.

Fig. 2(a) shows the absorption coefficient of F8T2, PC[60]BM, and PC[70]BM. All materials, F8T2, PC[60]BM, and PC[70]BM, contribute to the absorption within the blend. It can be seen that the absorption peak of F8T2 locates at 470 nm with an absorption coefficient of 1.63×10^5 cm^{-1}. Typical absorption bands at 330 nm for PC[60]BM and 370 and 460 nm for PC[70]BM are found [19,22].

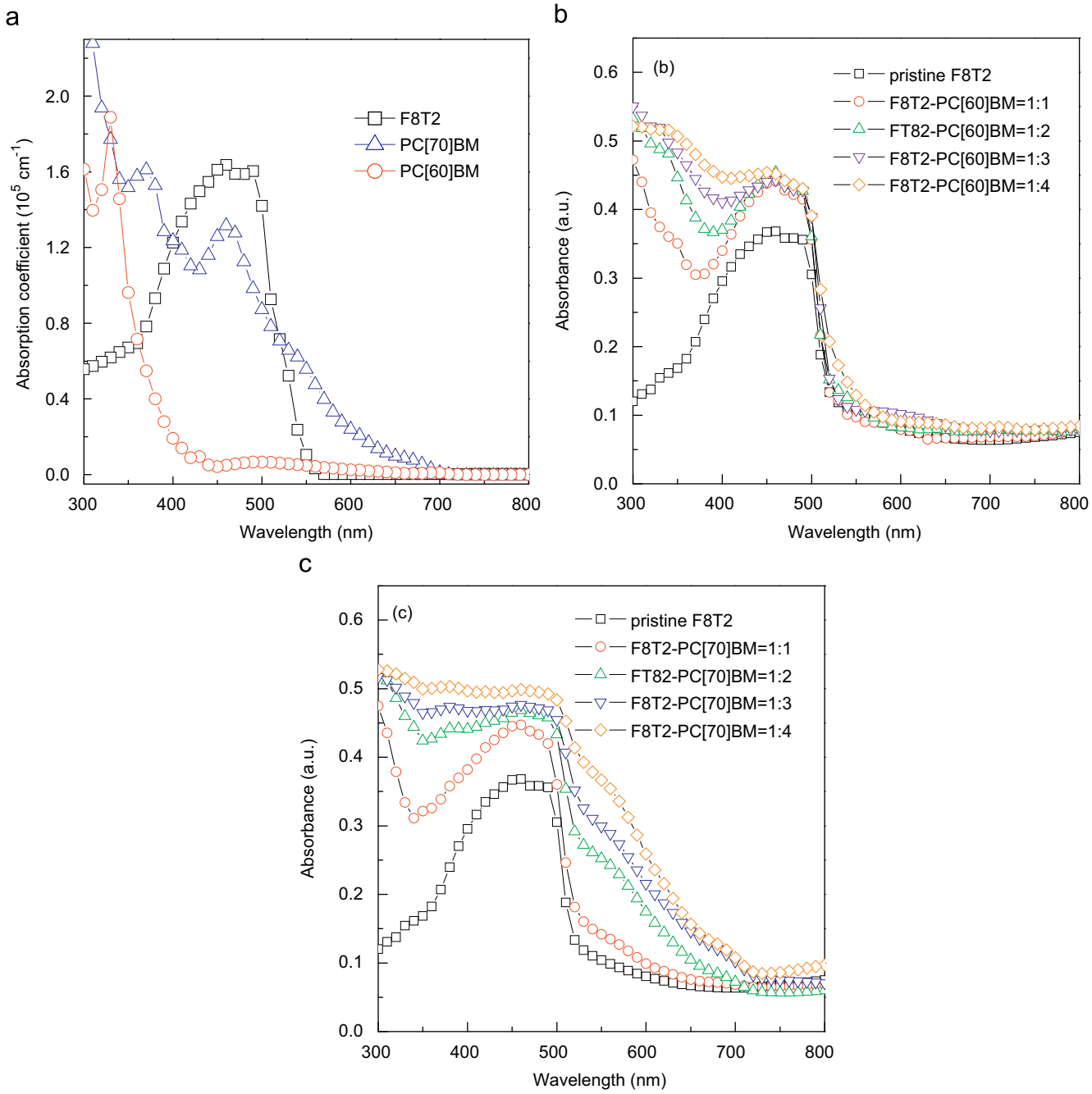

Fig. 2. (a) The absorption coefficient of F8T2, PC[60]BM, and PC[70]BM. UV–visible absorption spectra of the blended films in various ratios, (b) F8T2:PC[60]BM and (c) F8T2:PC[70]BM.

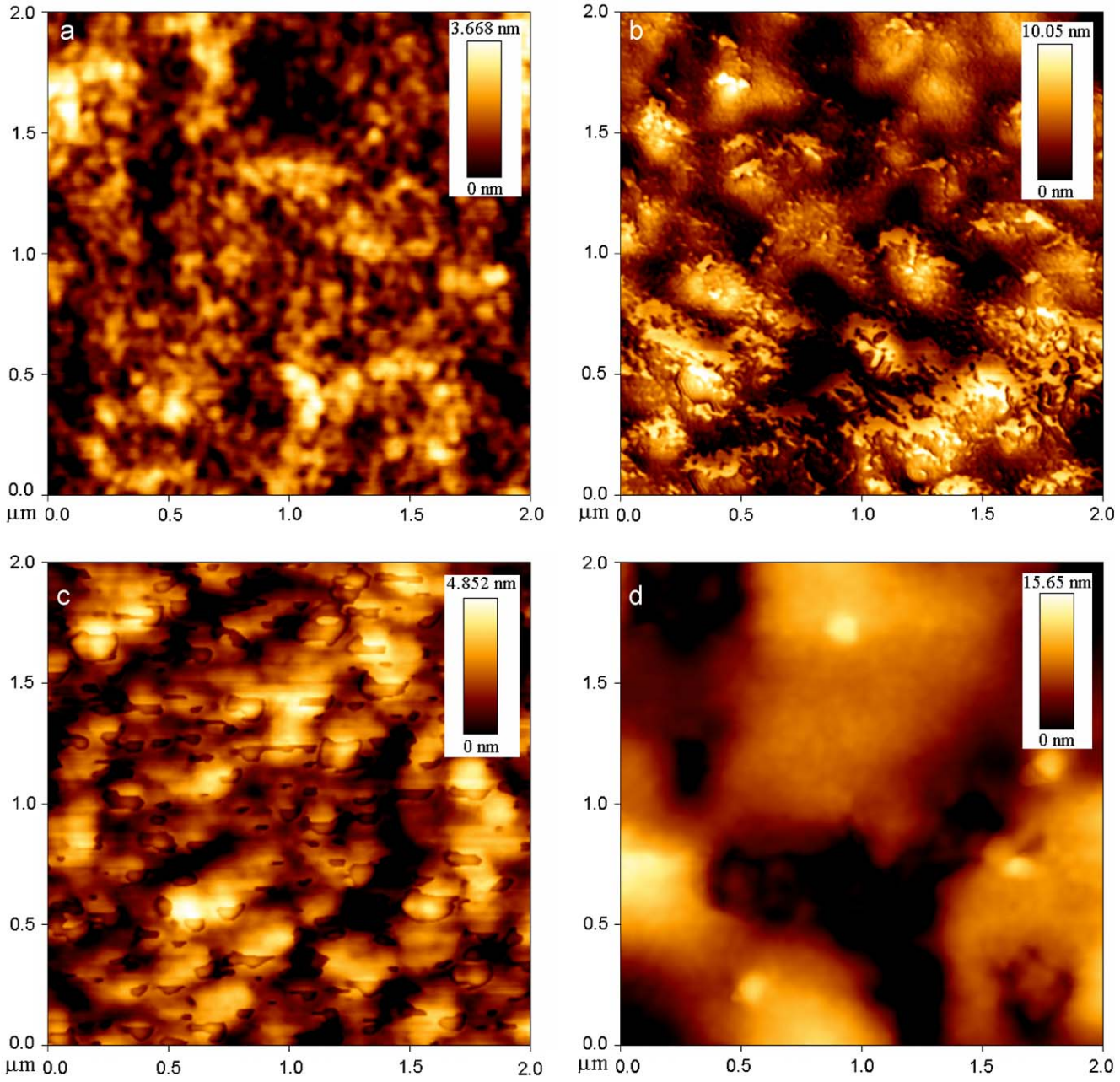

Fig. 3. AFM images of the blended films in various ratios (a) F8T2:PC[60]BM (1:1), (b) F8T2:PC[60]BM (1:4), (c) F8T2:PC[70]BM (1:1), and (d) F8T2:PC[70]BM (1:4).

The significantly higher absorption coefficient of PC[70]BM compared with that of PC[60]BM in the visible region is most relevant for the application in photodiodes, photodetectors, and photovoltaics. Fig. 2(b) and (c) shows the UV–visible absorption spectra of pristine F8T2 and their blend films with PC[60]BM and PC[70]BM at various weight ratios, respectively. Pure F8T2 reveals a broad absorption band located at 470 nm. The large band gap (2.4 eV) of F8T2 renders its absorption blue-shifted compared with P3HT. This feature makes it a limited light absorber. However, the absorption of F8T2 can be complemented by blending with PC[70]BM which shows strong absorption between 400 and 600 nm [23]. It appears that the absorption between 300 and 500 nm of F8T2 can be enhanced by blending with both PC[60]BM and PC[70]BM. But in the long wavelength region of 500–700 nm, where PC[60]BM is very close to transparent, PC[70]BM still shows a significant absorption. Hence, a better match with sun radiation is observed for F8T2:PC[70]BM. As a result, higher current density was obtained which is explained in the subsequent sections.

Fig. 3 shows the AFM images for the composite F8T2:PC[60]BM (Fig. 3(a) and (b)) and F8T2:PC[70]BM films (Fig. 3(c) and (d)). It has been found that the surface of F8T2:PC[70]BM films is quite rough compared with F8T2:PC[60]BM films. The former films have a root mean square roughness of 2.2 nm, compared with 1.3 nm for the latter films. The image of film blended with PC[60]BM (50 wt%) reveals a more homogeneous blend without obvious separate domains, while the PC[70]BM-based film (50 wt%) shows a separate domains with feature size of 250–300 nm. This indicates that the PC[70]BM blend film formed vertical phase separation which dramatically increases ordering of

F8T2 and facilitates the charges to move towards the respective electrodes and reduce the recombination, leading to improved photocurrent generation with respect to the PC[60]BM blend film. An unfavorable morphology of both the PC[60]BM and PC[70]BM blend films can be observed with higher ratios of fullerene to F8T2. When the PCBM ratio increases to 80%, the domain sizes of the composite films are approximately increased to 300–350 and 500–550 nm for PC[60]BM and PC[70]BM, respectively. Therefore, they provided less junction interface for exciton dissociations, leading to a decrease in photocurrent generation.

Fig. 4 shows the measured device operating parameters J_{SC}, PCE, V_{OC}, and FF as a function of fullerene weight ratios. A value of $J_{SC} = 5.28\,mA/cm^2$ for the F8T2:PC[70]BM (1:2.5) device is observed which is an increase of over 50% with respective to an optimized F8T2:PC[60]BM (1:1.5) cell. Although a non-uniform mix of constituents is observed in the films based on F8T2:PC[70]BM (1:2.5) which can lead to a poor charge separation, the photocurrent is still larger enough, indicating the excitation of PC[70]BM also contributes to the photocurrent. In these cases, the measured values of J_{SC} and PCE show an increase and then decrease with a larger fullerene weight ratios as shown in Fig. 4(a) and (b), respectively. This means that a higher fullerene weight ratio leads to more phase separation between donor and acceptor, thus enhancing the charge transport. However, a larger fullerene weight ratio tends to be less soluble, and leading to a serious aggregation of the fullerene which influences the charge separation as shown in Fig. 3. Furthermore, a strongly unbalanced charge transport can also be expected due to a large fullerene ratio, which, in turn, decreases the photocurrent due to the build up of the space charge at the interface. Hence, both the J_{SC} and PCE

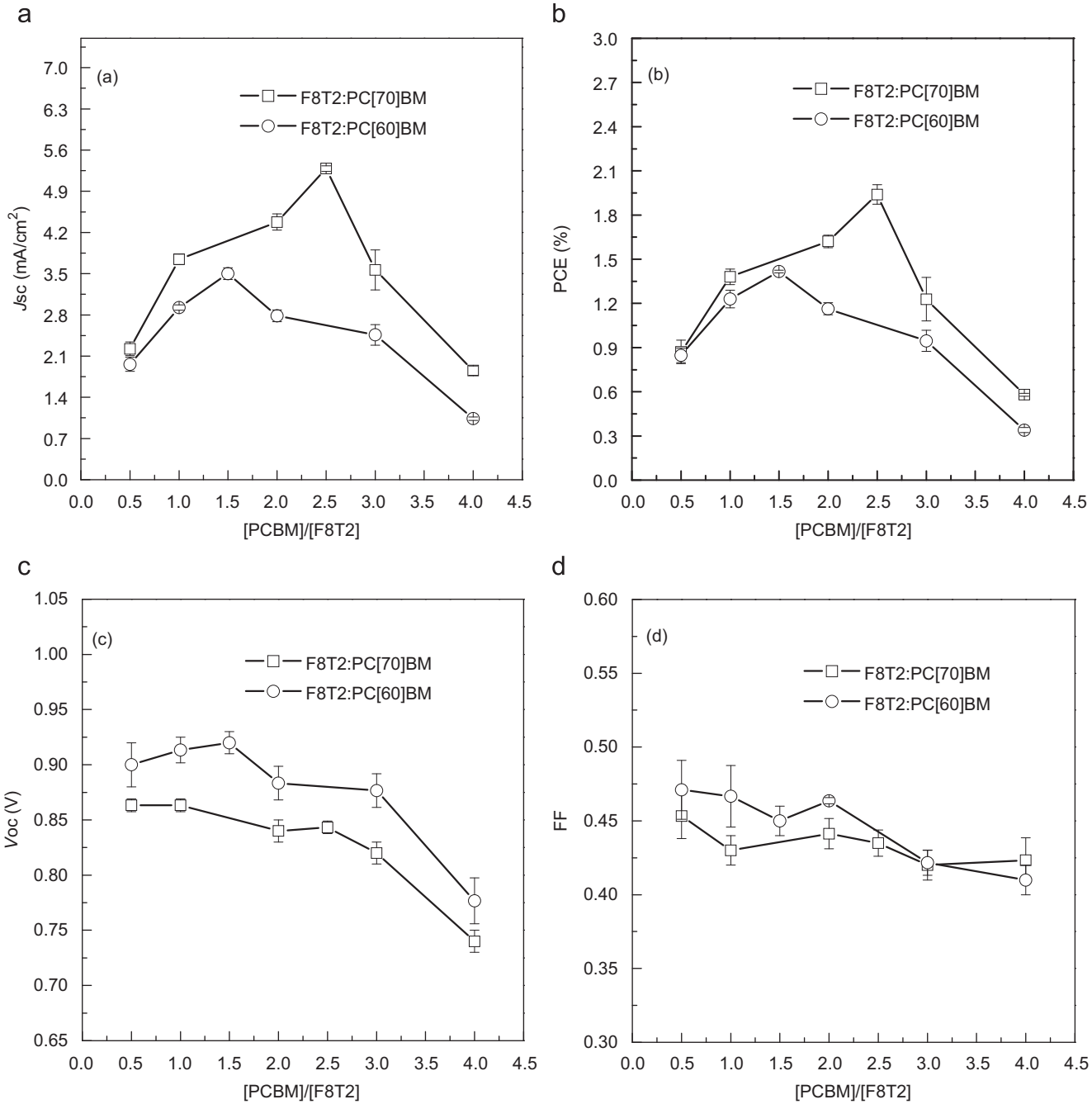

Fig. 4. Plots of J_{SC}, V_{OC}, FF, and PCE as a function of the blending ratios of fullerenes to F8T2.

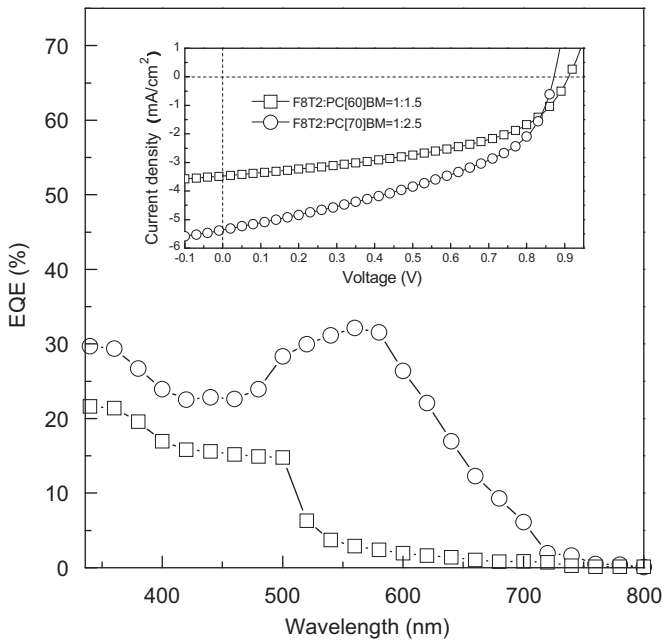

Fig. 5. EQE spectra of F8T2 blended with PC[60]BM (1:1.5) and PC[70]BM (1:2.5) devices. (Inset: corresponding *J–V* characteristics.)

decrease with larger fullerene weight ratios based on the two reasons described above. It is worthy to note that the maxima in the PCE and J_{SC} of the F8T2:PC[60]BM and F8T2:PC[70]BM solar cells are observed at the fullerene concentration equaling to 60 and 71 wt%, respectively. This strongly manifests that the improved performance of F8T2:PC[70]BM solar cell, compared with the one based on the analogous F8T2:PC[60]BM, is mainly due to its significantly broader and stronger absorption, which resulted in a higher photocurrent. Although the photocurrent can be enhanced by replacing of PC[60]BM with PC[70]BM, the V_{OC} values are observed to be slightly smaller. The V_{OC} diminishes as a result of the slightly larger LUMO energy of PC[70]BM, leading to a narrow energy difference between $HOMO^{F8T2}$ and $LUMO^{PC[70]BM}$ [24]. On the other hand, the V_{OC} and FF show a quite distinct behavior with various fullerene weight ratios compared with the cases of PCE and J_{SC}. The values for V_{OC} and FF vary monotonically with increasing fullerene content in the BHJ films. This can be rationalized by the incomplete charge generation and transport resulted from the aggregation of the large amount of fullerenes [25]. The miscibility of PC[60]BM with F8T2 is better than that of PC[70]BM; therefore, a better junction interface can be expected for F8T2:PC[60]BM just as indicated in Fig. 3. This leads to a slightly higher FF for F8T2:PC[60]BM compared with PC[70]BM as shown in Fig. 4(c) and (d), respectively. The smaller V_{OC} value of PC[70]BM is expected to be the result of a smaller LUMO energy which PC[70]BM possesses. The best cell has an active layer thickness of about 230 nm, containing 71 wt% of PC[70]BM with a J_{SC} of 5.28 mA/cm^2, a V_{OC} of 0.84 V , a FF of 0.44, and a PCE of 2.0%.

Fig. 5 shows the results of EQE measurements for F8T2 blended with PC[60]BM and PC[70]BM. The measured devices were fabricated with the best weight ratios of 1.5 and 2.5 for PC[60]BM and PC[70]BM, respectively. The inset is the *J–V* characteristics under illumination for the as-fabricated device which show a larger photocurrent for PC[70]BM-based device, as compared with that of PC[60]BM. The EQE of PC[60]BM-based device shows a maximum of 21.6% at a wavelength of 340 nm and decreases dramatically after 500 nm which is consistent with the absorption data. On the other hand, for the PC[70]BM-based device, the EQE maximum increases by a factor of 1.5, reaching 32.1% at 560 nm. Furthermore, the EQE stretches over the wavelength range of 500–700 nm which is wider than the PC[60]BM-based device. The increase in EQE is in good agreement with the absorption data of F8T2:PC[70]BM. This indicates that the excitation of PC[70]BM also contributes to the photocurrent.

4. Conclusion

In summary, it has been demonstrated that BHJ solar cells with a PCE value of 2.0% were achieved by applying a superior electron acceptor PC[70]BM to replace PC[60]BM for F8T2. A broader absorption spectrum in F8T2:PC[70]BM film covers the visible solar spectrum, resulting in a broader photocurrent response. Based on these findings, F8T2 is a potential candidate for assembling a tandem cell with other low bandgap polymers to cover the solar spectrum.

Acknowledgements

The authors are grateful to the National Science Council (NSC), Taiwan, under Grant nos. NSC 97-2120-M-002-012 and NSC 96-2221-E-001-017-MY2, and the Thematic Project of Academia Sinica, Taiwan for financial support.

References

[1] M. Wang, X. Wang, Electrodeposition zinc-oxide inverse opal and its application in hybrid photovoltaics, Sol. Energy Mater. Sol. Cells 92 (2008) 357–362.
[2] W.L. Ma, C.Y. Yang, X. Gong, K. Lee, A.J. Heeger, Thermally stable, efficient polymer solar cells with nanoscale control of the interpenetrating network morphology, Adv. Funct. Mater. 15 (2005) 1617–1622.
[3] J.H. Huang, Z.Y. Ho, D. Kekuda, C.W. Chu, K.C. Ho, Controlled growth of nanofiber network hole collection layers with pore structure for polymer–fullerene solar cells, J. Phys. Chem. C 112 (2008) 19125–19130.
[4] X.J. Wang, E. Perzon, J.L. Delgado, P. de la Cruz, F.L. Zhang, F. Langa, M. Andersson, O. Inganas, Infrared photocurrent spectral response from plastic solar cell with low-band-gap polyfluorene and fullerene derivative, Appl. Phys. Lett. 85 (2004) 5081–5083.
[5] L.M. Campos, A. Tontcheva, S. Gunes, G. Sonmez, H. Neugebauer, N.S. Sariciftci, F. Wudl, Extended photocurrent spectrum of a low band gap polymer in a bulk heterojunction solar cell, Chem. Mater. 17 (2005) 4031–4033.
[6] M.C. Scharber, D. Wuhlbacher, M. Koppe, P. Denk, C. Waldauf, A.J. Heeger, C.L. Brabec, Design rules for donors in bulk-heterojunction solar cells—towards 10% energy-conversion efficiency, Adv. Mater. 18 (2006) 789–794.
[7] H. Sirringhaus, T. Kawase, R.H. Friend, T. Shimoda, M. Inbasekaran, W. Wu, E.P. Woo, High-resolution inkjet printing of all-polymer transistor circuits, Science 290 (2000) 2123–2126.
[8] S.P. Li, C.J. Newsome, D.M. Russell, T. Kugler, M. Ishida, T. Shimoda, Friction transfer deposition of ordered conjugated polymer nanowires and transistor fabrication, Appl. Phys. Lett. 87 (2005) 062101-1–062101-3.
[9] N. Blouin, A. Michaud, M. Leclerc, A low-bandgap poly(2,7-carbazole) derivative for use in high-performance solar cells, Adv. Mater. 19 (2007) 2295–2300.
[10] W. Mammo, S. Admassie, A. Gadisa, F. Zhang, O. Inganäs, M.R. Andersson, New low band gap alternating polyfluorene copolymer-based photovoltaic cells, Sol. Energy Mater. Sol. Cells 91 (2007) 1010–1018.
[11] M. Sun, L. Wang, X. Zhu, B. Du, R. Liu, W. Yang, Y. Cao, Near-infrared response photovoltaic device based on novel narrow band gap small molecule and PCBM fabricated by solution processing, Sol. Energy Mater. Sol. Cells 91 (2007) 1681–1687.
[12] P.L.T. Boudreault, A. Michaud, M. Leclerc, A new poly(2,7-dibenzosilole) derivative in polymer solar cells, Macromol. Rapid Commun. 28 (2007) 2176–2179.
[13] A. Gadisa, W. Mammo, L.M. Andersson, S. Admassie, F. Zhang, M.R. Andersson, O. Inganas, A new donor–acceptor–donor polyfluorene copolymer with balanced electron and hole mobility, Adv. Funct. Mater. 17 (2007) 3836–3842.
[14] E.G. Wang, L. Wang, L.F. Lan, C. Luo, W.L. Zhuang, J.B. Peng, Y. Cao, High-performance polymer heterojunction solar cells of a polysilafluorene derivative, Appl. Phys. Lett. 92 (2008) 033307-1–033307-3.
[15] J.H. Huang, Z.Y. Ho, D. Kekuda, Y. Chang, C.W. Chu, K.C. Ho, Effects of nanomorphological changes on the performance of solar cells with blends of poly[9,9'-dioctyl-fluorene-*co*-bithiophene] and a soluble fullerene, Nanotechnology 20 (2009) 025202–025211.

[16] J.H. Huang, C.Y. Yang, Z.Y. Ho, D. Kekuda, M.C. Wu, F.C. Chien, P. Chen, C.W. Chu, K.C. Ho, Annealing effect of polymer bulk heterojunction solar cells based on polyfluorene and fullerene blend, Org. Electron. 10 (2009) 27–33.
[17] S. Rait, S. Kashyap, P.K. Bhatnagar, P.C. Mathur, S.K. Sengupta, J. Kumar, Improving power conversion efficiency in polythiophene/fullerene-based bulk heterojunction solar cells, Sol. Energy Mater. Sol. Cells 91 (2007) 757–763.
[18] J. Jo, D. Vak, Y.Y. Noh, S.S. Kim, B. Lim, D.Y. Kim, Effect of photo- and thermo-oxidative degradation on the performance of hybrid photovoltaic cells with a fluorene-based copolymer and nanocrystalline TiO_2, J. Mater. Chem. 18 (2008) 654–659.
[19] M.M. Wienk, J.M. Kroon, W.J.H. Verhees, J. Knol, J.C. Hummelen, P.A. van Hal, R.A.J. Janssen, Efficient methano[70]fullerene/MDMO-PPV bulk heterojunction photovoltaic cells, Angew. Chem. Int. Ed. 42 (2003) 3371–3375.
[20] X.J. Wang, E. Perzon, F. Oswald, F. Langa, S. Admassie, M.R. Andersson, O. Inganas, Enhanced photocurrent spectral response in low-bandgap polyfluorene and C70-derivative-based solar cells, Adv. Funct. Mater. 15 (2005) 1665–1670.
[21] Y. Yao, C.J. Shi, G. Li, V. Shrotriya, Q.B. Pei, Y. Yang, Effects of C70 derivative in low band gap polymer photovoltaic devices: spectral complementation and morphology optimization, Appl. Phys. Lett. 89 (2006) 153507-1–153507-3.
[22] H. Hoppe, N. Arnold, N.S. Sariciftci, D. Meissner, Modeling the optical absorption within conjugated polymer/fullerene-based bulk-heterojunction organic solar cells, Sol. Energy Mater. Sol. Cells 80 (2003) 105–113.
[23] J.W. Arbogast, C.S. Foote, Photophysical properties of C70, J. Am. Chem. Soc. 113 (1991) 8886–8889.
[24] N. Matsuzawa, D.A. Dixon, Semiempirical calculations of the polarizability and second-order hyperpolarizability of fullerenes (C60 and C70), and model aromatic compounds, J. Phys. Chem. 96 (1992) 6241–6247.
[25] K.C. Kim, J.H. Park, O.O. Park, New approach for nanoscale morphology of polymer solar cells, Sol. Energy Mater. Sol. Cells 92 (2008) 1188–1191.